

Monitoring and Predicting Landuse/Landcover Change Using an Integrated Markov Chain & Multilayer Perceptron Models: A Case Study of Sahiwal Tehsil

Sharjee¹ Masud¹, Zahir Ali², Mateeul Haq², Badar Munir Ghuri¹

¹Department of Remote Sensing & GISc, Institute of Space Technology, Karachi, Pakistan

²Pakistan Space & Upper Atmosphere Research Commission (SUPARCO), Karachi, Pakistan

Abstract

Population growth, rapid developments and natural processes bring changes in landuse/landcover (LULC). The impact of these changes on natural resources and environment globally attract the researchers. The LULC changes has a great influence on agriculture, natural vegetation, and water resources. In this study, Remote Sensing (RS) and Geographical Information System (GIS) tools were employed instead of conventional methods. The target study area of Sahiwal tehsil comes under the jurisdiction of Sargodha district of Punjab province in Pakistan. A supervised classification (maximum likelihood) algorithm was applied on three Landsat TM images of 1999, 2009 and 2014. Five LULC classes including vegetation, built-up land, water, barren land and cultivated land were extracted. Furthermore, CA-MARKOV and MLP _MARKOV models were used for projecting LULC changes in the study area. The projected images of 2014 from both models were then compared with a base map of 2014 and MLP_MARKOV was selected for projecting 2019 LULC changes. The projected LULC classes for 2019 shows similar trends with an increasing trend in cultivated land.

Keywords: Landuse/Landcover Change, Markov Chain, Cellular Automata

1. INTRODUCTION

Land is a vital natural asset on which all measures for development are grounded. Landuse/landcover change is a significant factor for environmental and ecological change [1]. Local landuse/landcover changes in the consequences of environmental and ecological changes caused the recent global changes [2]. Landuse/landcover are two different terms. Landuse is an activity and development that people start on any type of landcover e.g. agriculture land, built up land. In contrast, landcover is a physical and organic cover of the land which includes water

body and vegetation [3]. As the population increases, the demand for agriculture, urban and industrial landuse also increases [4]. Growing population of the world causes the destruction of natural and X-ray radiations and due to intermittently owing to their expense, researchers largely depend on solar resources as well as the nature itself. Anthropogenic activities change the surface of the earth which consequently degrading the forest and vegetation cover [5]. Better management of urban areas requires comprehensive and effective monitoring of physical changes over time [6]. According to the United Nations (UN) and Population Reference Bureau-PRB (2000), world's population living in the urban areas will become five billion in the next three decades [7]. Due to increase in commercial as well as industrial activities in land, the physical state of land is extensively affected which in turn affects the environment. Therefore, information regarding landuse/landcover is essential for planning of different landuse schemes to fulfill the demand of increasing human population and getting knowledge about the landuse change.

From space, the observation of earth gives a brief view of landuse/landcover changes. Remote sensing technology is vital to understand the impact of anthropogenic activities and changes in natural resources. Due to rapid landuse/landcover change, the space borne information become more useful information for exploiting the earth resources [8]. Repetitive coverage of remote sensing satellites makes these instruments valuable for change detection study because it involves two or more imageries captured in two different periods [16]. Satellite imagery were used in the geospatial studies and other fields in last three decades for the policy and decision making. Satellite based data are essential for the study of urban and rural management and planning. It is used as a tool for landuse/landcover identification and classification of various features on the land surface[9]. Geographical information systems (GIS) and remote sensing are two separate technologies which are used in the modern era for natural resource management [10]. Landuse/landcover change can be analyzed and quantified by using the remote sensing and geographic information system [11, 12]. Landuse/landcover maps are prepared from the visual and digital interpretation of satellite dataset. This can be the input in GIS environment for analysis of change in landuse/landcover. This analysis provides a base for prediction of future landuse/landcover trends [13, 14]. Mapping and classification of landuse/landcover features which are recognizable are the main application of satellite remote sensing [15].

Change detection is a useful process for quantifying change in distribution of different landuse/landcover classes. Urban planners use satellite imagery for urban sprawl, change detection, management and several other applications [16, 17, 18]. Predicting future landuse/landcover development is an important tool to estimate the vulnerabilities in landscape ecology. Recent developments and pattern in landuse/landcover change trends are main inputs in modeling urban growth [19]. Types of landuse/landcover, its locations, pace of changes and effects of driving forces are interesting information for decision and policy makers. It can obtain information from different landuse/landcover models. On the basis of past landuse/landcover pattern, these models forecast spatial distribution of landuse/landcover classes. [20].

In this study, three landuse/landcover maps of 1999 and 2009 and 2014 were generated. The 1999 and 2009 classified maps were then used as input of CA_Markov and MLP_Markov modular in order to predict the landuse/landcover map of 2014. For model selection, kappa

statistic has been used. Based on overall kappa statistics MLP_Markov has been used for prediction of 2019 landuse/landcover map.

2. Methodology

The following flow chart explains the methodological framework for carrying out this research work.

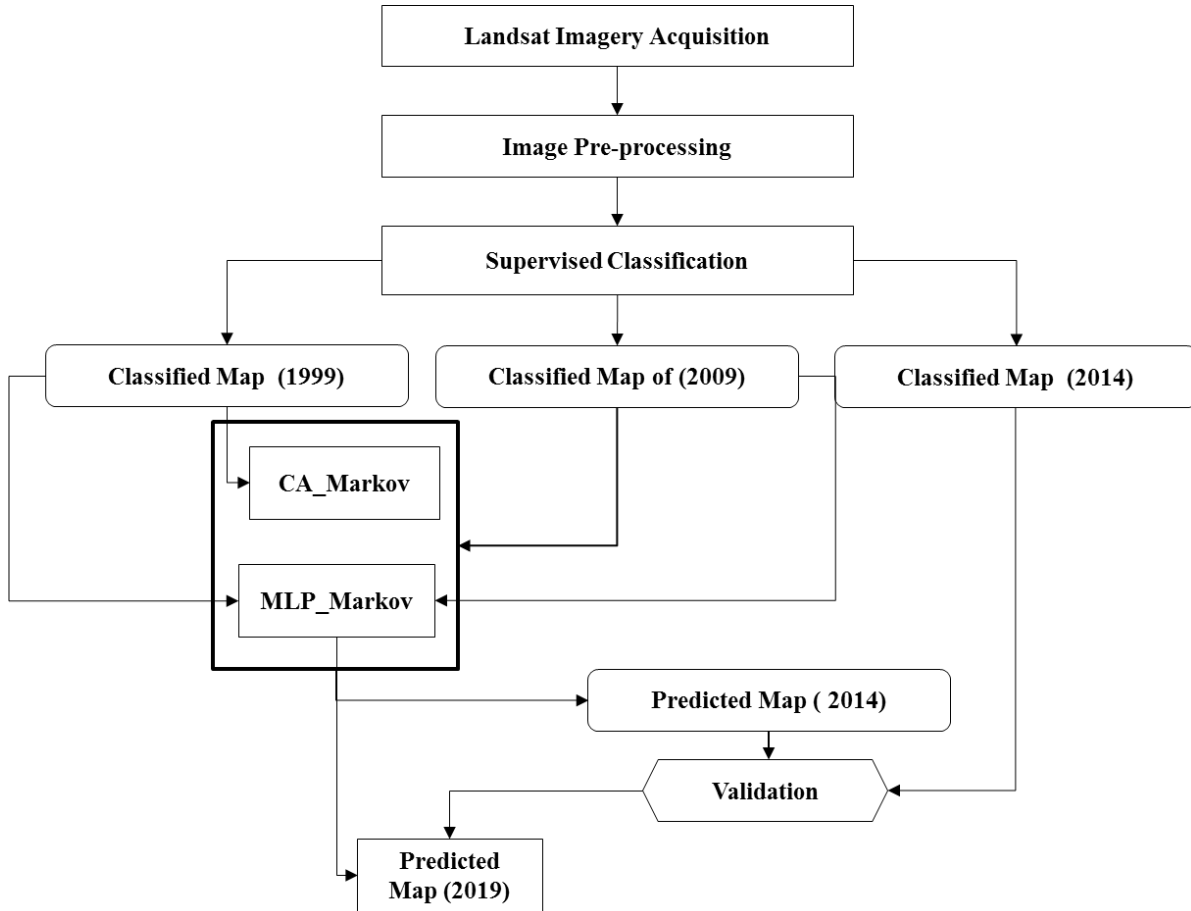


Figure 1: Flow chart for organization of data

Two Landsat TM (Thematic Mapper) and one Landsat 8 images having row/path 150/38 were acquired. These images belonged to three different periods 1999, 2009 and 2014. Prior knowledge and brief survey of the study area further helped in extracting landuse/landcover categories which are;

1. Vegetation.
2. Built-up land
3. Barren land
4. Water
5. Cultivated land

In this study, the training signatures (samples) were collected from images of 1999, 2009 and 2014. Training signatures comprise of polygons or rectangles as a group of pixels on the image. This group of pixels had homogeneous spectral characteristics. Training sample polygons were delineated by region growing properties tool in EDRAS IMAGIN software. In this study, 150 training samples were collected from each imagery and stored in signature editor. Maximum likelihood classifier was used to classify these images.

Markov Chain Analysis is used to forecast the change in landuse/landcover classes between two stages or periods. It is a process in which the future state of a landuse/landcover class can be modeled on the basis of the immediately previous state.

3. Study Area

Sahiwal is a Tehsil of Sargodha District in Punjab province. It lies between 31.6964280 N to 32.0589650 N and 72.1922840 E to 72.5791610 E. Sahiwal tehsil is situated in the southern west of Sargodha district. According to the 1998 census, the population is 236,000. Constitute of male population is 119,638 and female are 116,585. The tehsil consists of 14 Union Councils. The average high temperature is 39°C in summer while the average low temperature is 8°C whereas the average annual rainfall is 400 mm.

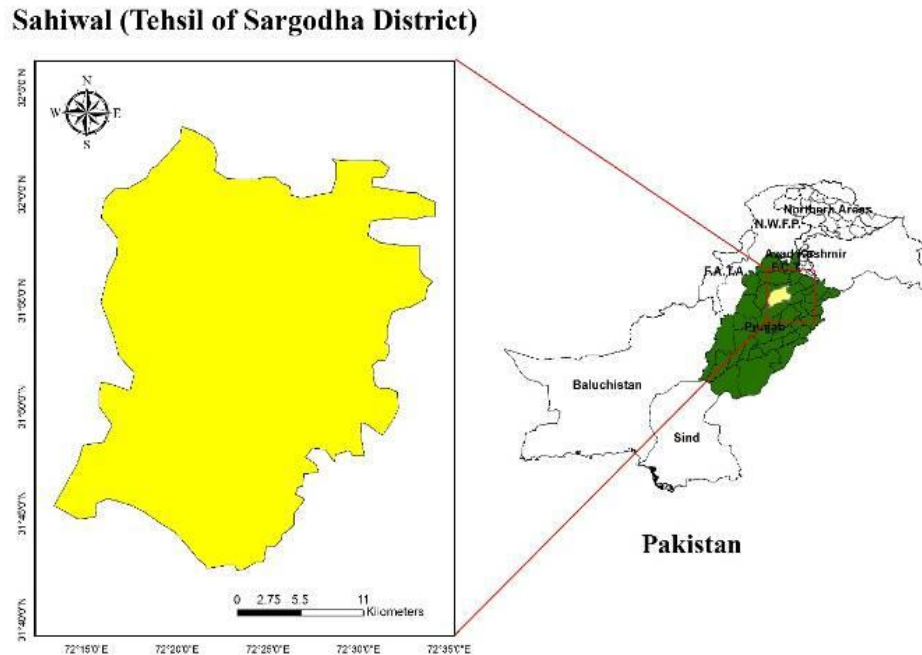


Figure 2: Study Area location (yellow) on provincial map

1. Results and Discussion

1.1 Change between 1999 – 2009

The classified maps for years 1999 and 2009 shown in Figure 3.

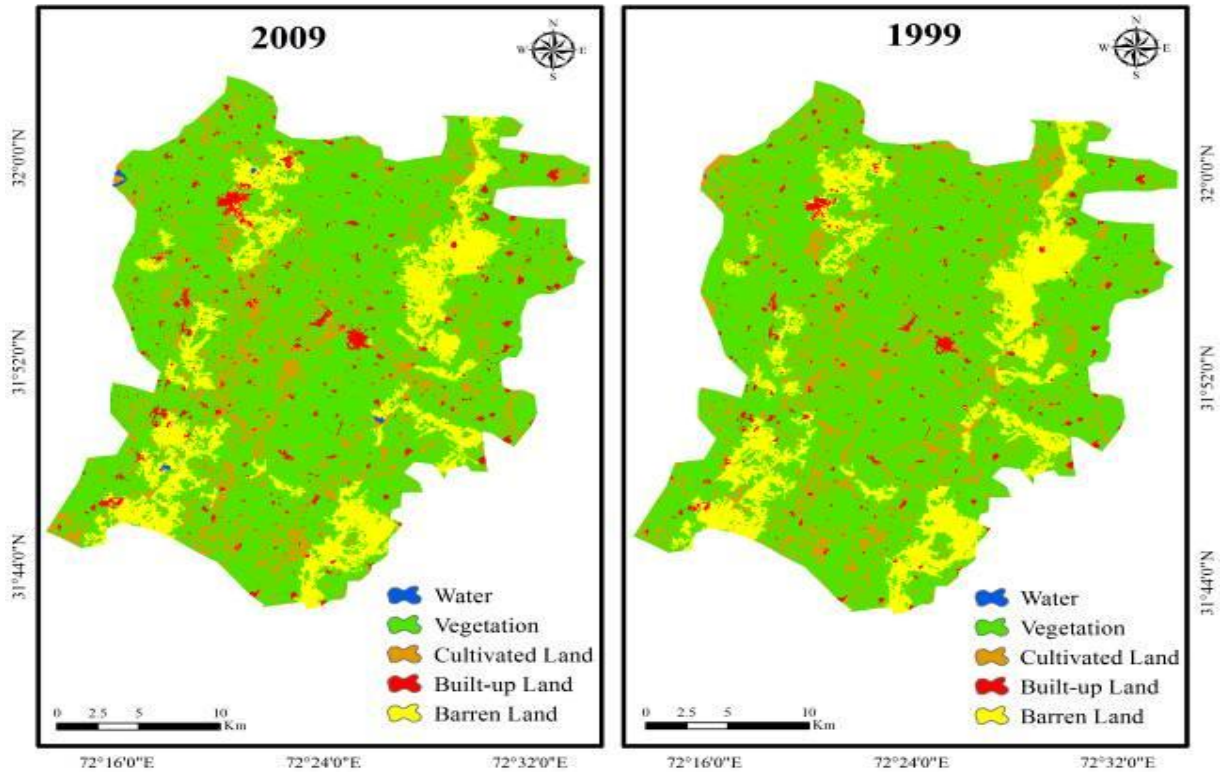


Figure 3: Landuse/Landcover classified map of 1999 and 2009

Table 1: Landuse/landcover classes of 1999 and 2009

Classes	Covered Area in 1999 (Sq.km)	Covered Area in 2009 (Sq.km)	Change in Sq.km
Vegetation	522.27	517.04	5.23
Built-up land	16.35	25.34	8.99
Barren land	111.71	109.49	2.41
Water	0.040	0.92	0.88
Cultivated land	108.94	106.53	2.22

Table 1 shows that vegetation (which include natural and agriculture area) has been decreased up to 5.24 sq.km. Built-up area has been increased by 8.99 sq.km which have effect on vegetation and cultivated area. Barren land has been decreased from 111.71 sq.km to 109.49 sq.km. Water

bodies which consist of canals, river channels and fish pounds have been increased from 0.040 sq.km to 0.92 sq.km. Cultivated land has been decreased from 108.94 to 106.53 sq.km.

4.2 Change between 2009 – 2014

The classified maps for the years 1999 and 2009 are shown in Figure 4.

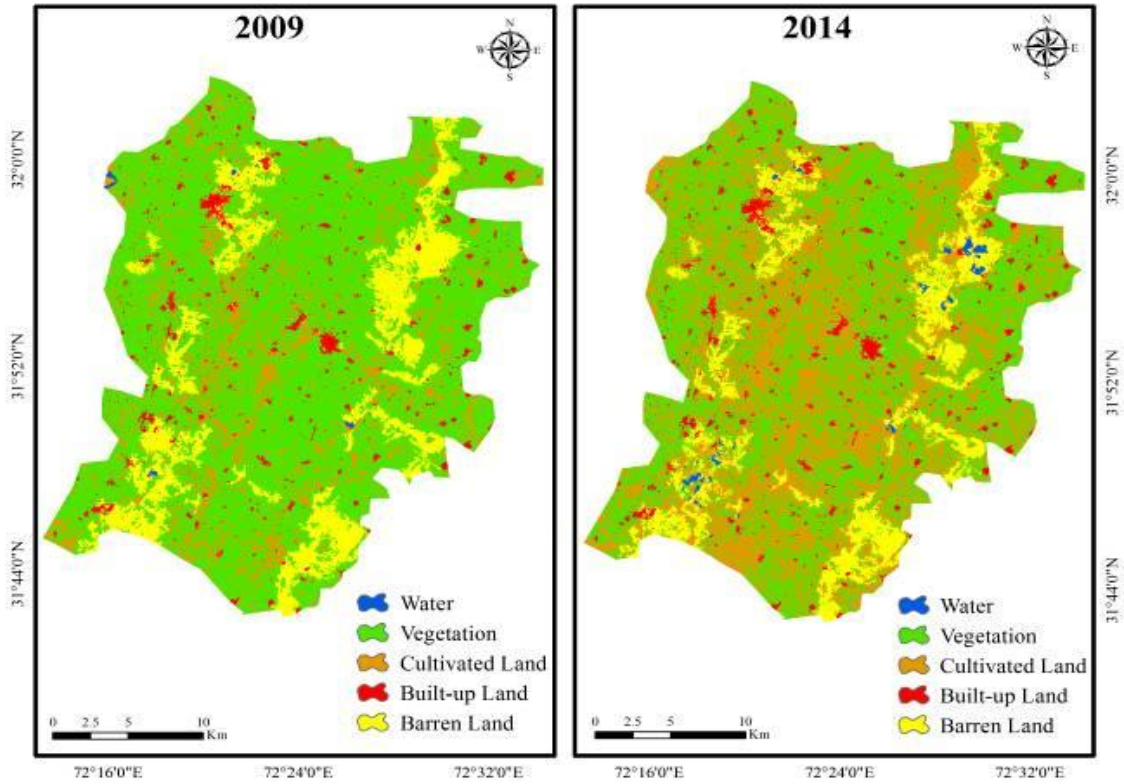


Figure 4: Landuse/landcover classified map of 2014

Table 2: Landuse/landcover classes of 2009 and 2014

Classes	Covered Area in 2009 (Sq.km)	Covered Area in 2014 (Sq.km)	Change in Sq.km
Vegetation	517.04	337.26	179.77
Built-up land	25.34	28.21	2.88
Barren land	109.49	91.40	8.10
Water	0.92	4.15	3.23
Cultivated land	106.53	298.30	191.76

Table 2 shows that area covered by vegetation has been decreased up to 179.77 sq.km. The reason behind this difference was seasonal variation. Former image was captured in February

2009 in which crop is at peak. While the later image was captured in April 2014 from which crop start harvesting. The Built-up area has been increased by 2.88 which also have effect on vegetation and cultivated area. Barren land has been decreased from 109.49 sq.km to 91.39 sq.km. Water bodies have been increased from 0.92 sq.km to 4.14 sq.km. Cultivated land has been increased from 106.53 sq.km to 298.29 sq.km.

4.3 Transition Probability Matrix

MARKOV Modular in IDRIDI taiga was used to generate transition probability matrix. The transition probability matrix archives the probability of each landuse/landcover category that will change into the other category. Two landuse/landcover maps of 1999 and 2009 were used as an input in MARKOV Modular to originate the transition probability matrix.

Table 3: Transition probability matrix for 2009 to 2019

Classes	Vegetation	Built-up land	Cultivated land	Water	Barren Land
Vegetation	0.7522	0.0081	0.2029	0.0003	0.0366
Built-up land	0.0468	0.8459	0.0486	0.0000	0.0587
Cultivated Land	0.5161	0.0156	0.4410	0.0014	0.0259
Water	0.0000	0.0000	0.3577	0.6423	0.0000
Barren land	0.1863	0.0233	0.0285	0.0069	0.7550

In the above 5 by 5 matrix rows represented the LULC classes of the earlier satellite image of 2009. On the other hand, columns represented the later projected satellite image of 2019. The probabilities presented in the above table 3 showed that vegetation has a probability of 0.7522 to be remained same as vegetation in 2014 and 0.0081 probability to be changed into built-up land, 0.2029 to cultivated land, 0.0003 to water, and 0.0366 to land. Similarly, the built-up area has a probability of 0.8459 to be remained as built-up in the projected year of 2019, 0.0468 changes into vegetation, 0.0486 to cultivated land, 0.0000 to water and 0.0366 to barren land.

Cultivated land has a probability of 0.4410 to be remained as barren land, 0.5161 changed to vegetation, 0.0156 changed into the built-up land, 0.0014 into the water and 0.0259 to barren land. Water has a probability of 0.6423 to be remained as water in next 10 years and barren land has a probability of 0.7550 to be remained as same class. Hence built-up area has the maximum probability to remain in same class and cultivated land shows minimum probability to remain in same class.

4.4 Cellular Automata

John von Neumann was the inventor of cellular automata, it constitutes discrete cellular space model complex behaviors grounded on transition rules [22]. CA model comprised of four components.

1. Cell space
2. States
3. Neighborhood
4. Transition rules

The state of each cell in an array at any time (t+1) depends upon its own state at any time (t) and state of nearby cells at any time (t).

4.5 Cellular Automata and Markov chain analysis (CA_MARKOV) model

In Markov model, the amount of difference of each class in time t(0) and t(1) determine the extent of LULC class at time t(2) and output is a non- spatial probability matrix [23]. Cellular Automata adds the spatial dimensions in Markov chain.

LULC map of time (t2), suitability maps and a contiguity filter were inputs of CA_Markov. At the beginning of the iterative process, determination of total number of iterations is essential that will be applied to predict future scenario. Generally, after executing each iteration, each LULC category, gain or lose some of its lands to one or more other LULC category.

In this respect, the process divides landcover map into two classes: host and claimant class [24]. Each claimant class takes lands from the host class, host classes can be one or more. Claimant class chose to land on the basis of suitability maps. Multi-Objective Land Allocation (MOLA) algorithm provide the option for handling the competition for specific land parcels between claimant classes [25].

Suitability maps, contiguity filter and ranking determine gain or loss of land between claimant and host classes. All above operations have been done in IDRISI taiga [23]. Markov model applies contiguity rule for a pixel near to a vegetation area is most likely to be transformed into vegetation area [23]. A 5×5 mean contiguity filter has been applied to this study.

This contiguity filtering has been used for suitability images of each LULC class. The pixels of one landcover category exist in the neighborhood, increases the suitability value for that particular landcover type. In another way, the pixel value remains the same [23].

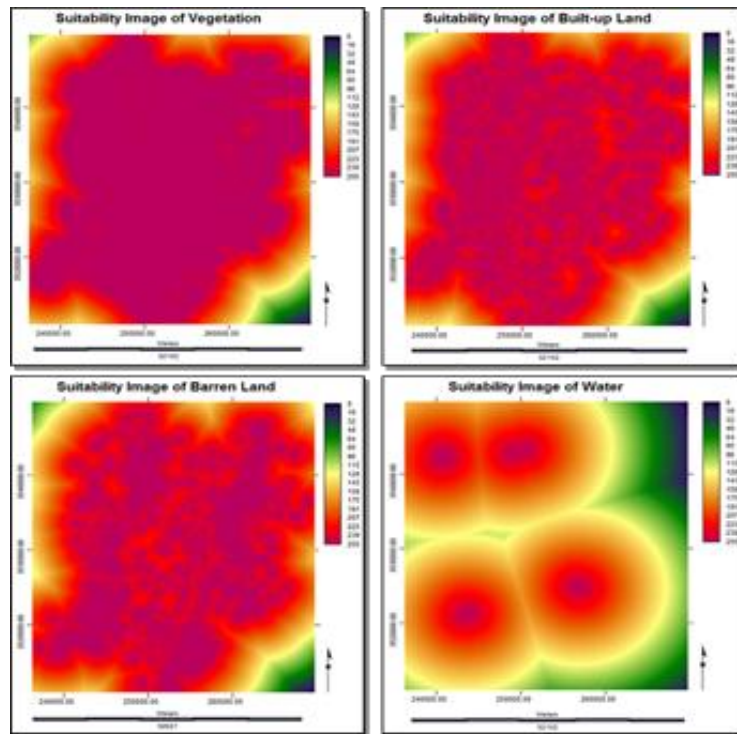
4.6 Preparation of Suitability Maps

It is difficult task to prepare suitability maps for each LULC category because different types of information and data are required. To integrate all sorts of constraints and factors that exist inside the area of interest is difficult. Therefore, a simple supposition to standardize fuzzy factor of that pixel nearer to an existing LULC category has the highest suitability. Pixel exists completely inside built-up contain highest suitability value denoted by (255) and pixels distant from existing built-up pixels contain less suitability values. Lowest suitability values pixels will be those farthest away from built-up land. Now the suitability of pixel for particular category decreases with distance. Linear distance decay function is suitable for this study. It assists the basic idea of proximity. In future, a pixel adjacent to a vegetation has more likelihood to convert into vegetation area. Although this concept is not always ideal in case of the vegetation and water situation.

There are three types of Fuzzy membership functions The Sigmoidal, J-shaped, and Linear. Out of these type linear is used here. The fuzzy set analysis controls shape of the curve. The positions of 4 inflection points a, b, c, d are input in the fuzzy set analysis.

The linear function has three shapes monotonically increasing, symmetric and decreasing functions. This curve begins at the inflection point "c" where value starts from (255) then falls and stays at the inflection point "d" where value becomes (0). "Monotonically Decreasing" Linear function has been selected for this study because it meets the basic supposition. For each landcover type at the earlier stage, the Boolean images (2009) have been prepared. The area of interest is represented by value 1 where the area of no interest is shown by value 0. Distance images for each Boolean LULC produced. Distance images are important to measure the values of suitability. Euclidean distance function has been used to generate distance images [27].

From the distance images, lowest and highest values were identified. Fuzzy set membership analysis module in IDRISI Taiga used these values to produce suitability maps. For this study, since the linear function has been used 'c' is considered as the lowest value and the inflection point 'd' is considered as the highest value.



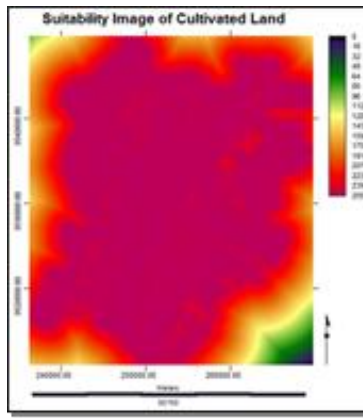


Figure 5: Suitability images of each landuse/landcover class (2009)

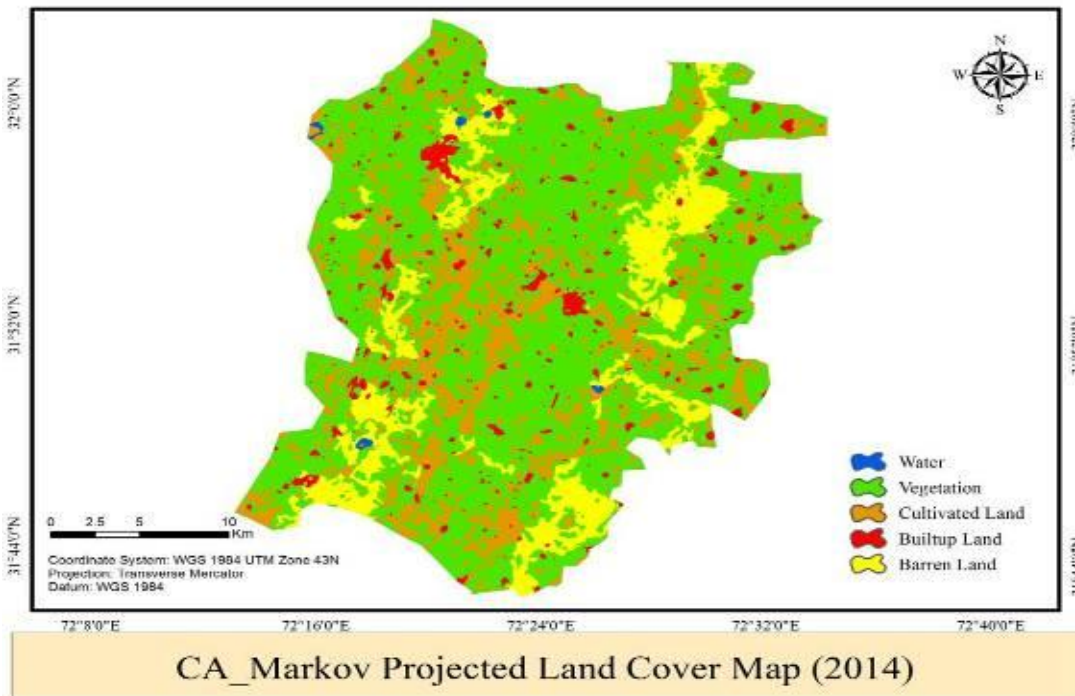


Figure 6: CA_Markov Landuse/Landcover Map for the year 2014

4.7 Multilayer Perceptron Model

Neurons which are called the perceptron are the basic elements of the multilayer perceptron. It consists of the input layer and output layer while hidden layers exist between output layers and input layers. Flow of data is unidirectional, from input to output. So this method is called feed forward method [27].

Mathematical notation is:

$$y = \varphi \left(\sum_{i=1}^n \omega_i x_i + b \right) = \varphi(w^T x + b)$$

where ω denotes the vector of weights, x is the vector of inputs, b is the bias and φ is the activation function.

4.8 Multi-Layer Perceptron Markov Modelling (MLP_MARKOV)

Multilayer perceptron Markov modeling is the combination of multilayer perceptron and Markov chain analysis. This type of LULC modeling is based on mapping the transition potential among LULC classes, for example, vegetation to built-up, barren to built-up, barren to water. MLP_MARKOV modeling consists of four stages, transition sub model development, testing explanatory variable and development of transition potentials maps. These transition potential maps have been used as an input in Markov chain model to simulate LULC change for future. But it is not necessary to consider all transitions. By considering the research purpose in this study the temporal changes in the built-up area was the main aim.

Therefore, only the transitions from, 'vegetation to built-up Area', barren land to the built-up area', water to built-up land and 'cultivated land to built-up area' have been considered. No transition from water to built-up land has occurred. Multilayer perceptron automatically has not considered it for transition mapping. To forecast the change empirically model each of above-mentioned transitions is essential. Multilayer perceptron offers an opportunity to model several transitions at once or separately. Before modeling the changes, it is essential to identify main driving or explanatory variables which have the impact of the change in the built-up land. Since new built-up land grows near existing built-up land. Hence variable 'distance all built-up land' has been selected as an input. Other variables 'distance from water bodies', 'distance from fallow land', 'distance from vegetation' and 'distance from barren land and the likelihood of changes of all LULC classes to built-up land have also taken as an input in transition sub model. Empirical likelihood image has been created by using LULC map of 1999 and 'transition map of all to built-up' in variable transformation method in IDRISI Taiga. Transition map has also been created in IDRISI. The categorical values in likelihood image point out the likelihood of pixels to changing into the built-up land. Higher values indicate increasing the likeliness of pixels to change into the built-up land.

For this study, Cramer's V has been used for measuring the association between driving variables and change. A value higher than 0.15 are considered useful and value less than 0.15 can be rejected. All selected variables have reasonable Cramer's V.

Modeling of transition potentials is next step on which MLP_MARKOV is based. Minimum 2515 cells go to transition from 1999 to 2009 and MLP automatically chosen 2515 cells as a sample size for training and testing. Default 10,000 iterations have been finished by MLP neural network RMS error has been smooth and decreased after finishing iteration. Three transition potential maps have been produced. The legend represents value from 0 to 1.

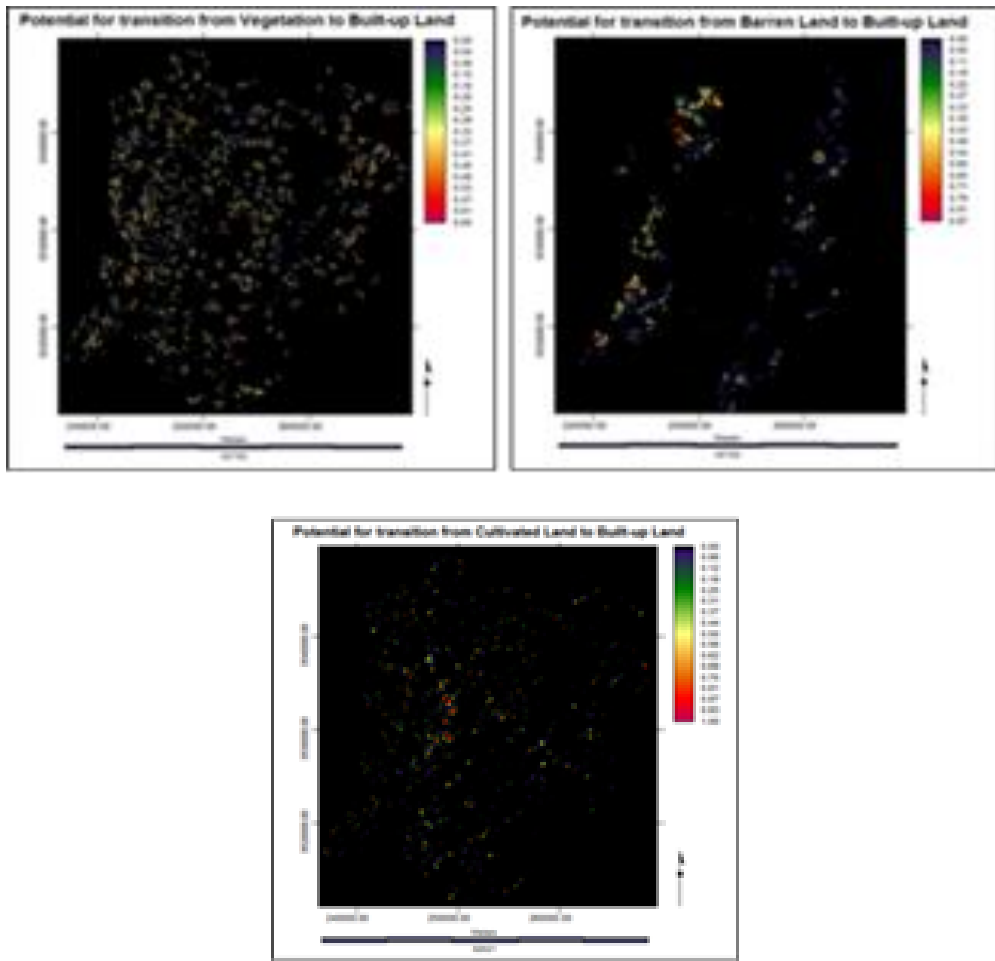


Figure 7: Transition Potential Maps (1999-2009)

MLP_MARKOV determine weights of transitions include in the matrix of probabilities. Markov chain analysis uses transition potential images for generation of simulated 2014 map. This combination of MLP and Markov has been called MLP_MARKOV.

Table 4: Transition Probabilities Grid for Markov Chain

Classes	Vegetation	Built-up land	Cultivated	Water	Barren
Vegetation	0.8849	0.0037	0.0942	0.0001	0.0170
Built-up land	0.0015	0.9952	0.0015	0.0000	0.0018
Cultivated land	0.4442	0.0135	0.5188	0.0012	0.0223
Water	0.0000	0.0000	0.2443	0.7557	0.0000
Barren land	0.0850	0.0106	0.0130	0.0031	0.8883

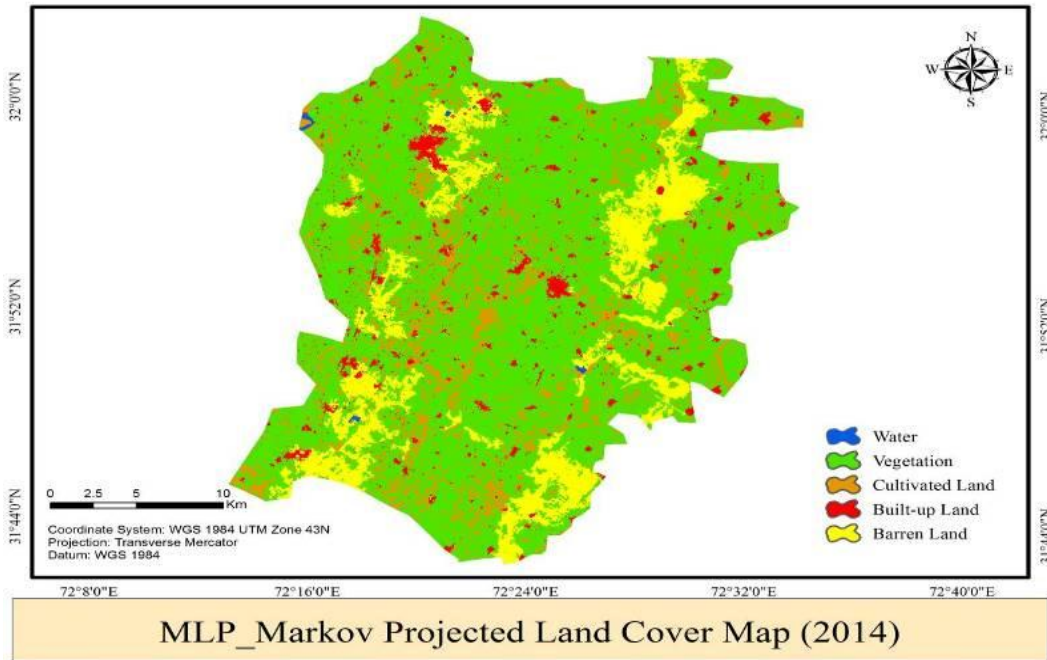


Figure 8: MLP_Markov Projected Landuse/landcover Map for the year 2014

4.9 Model Selection

kappa statistics divide into two statistics, kappa histo deals with quantitative similarity and kappa location represent location similarity among LULC map and projected map [28].

To predict future LULC two models have been employed. One is the most suitable model for this study which is selected based on kappa values. Overall kappa values of both models are low but MLP_MARKOV show relative high value (0.401).

Table 5: Per Category Kappa Statistics (CA_MARKOV)

CA_MARKOV for 2014	Per Category Values		
	Kappa	K Loc	K histo
Vegetation	0.301	0.448	0.671
Built-up land	0.817	0.841	0.971
Cultivated land	0.198	0.346	0.573
Water	0.205	0.361	0.567
Barren land	0.811	0.886	0.916
Overall kappa	0.387	0.554	0.698

Table 6: Per Category Kappa Statistics (MLP_MARKOV)

MLP_MARKOV for 2014	Per Category Values		
	Kappa	K Loc	K histo
Vegetation	0.310	0.565	0.549
Built-up land	0.886	0.912	0.971
Cultivated land	0.167	0.420	0.398
Water	0.174	0.482	0.361
Barren land	0.889	0.985	0.902
Overall kappa	0.401	0.683	0.587

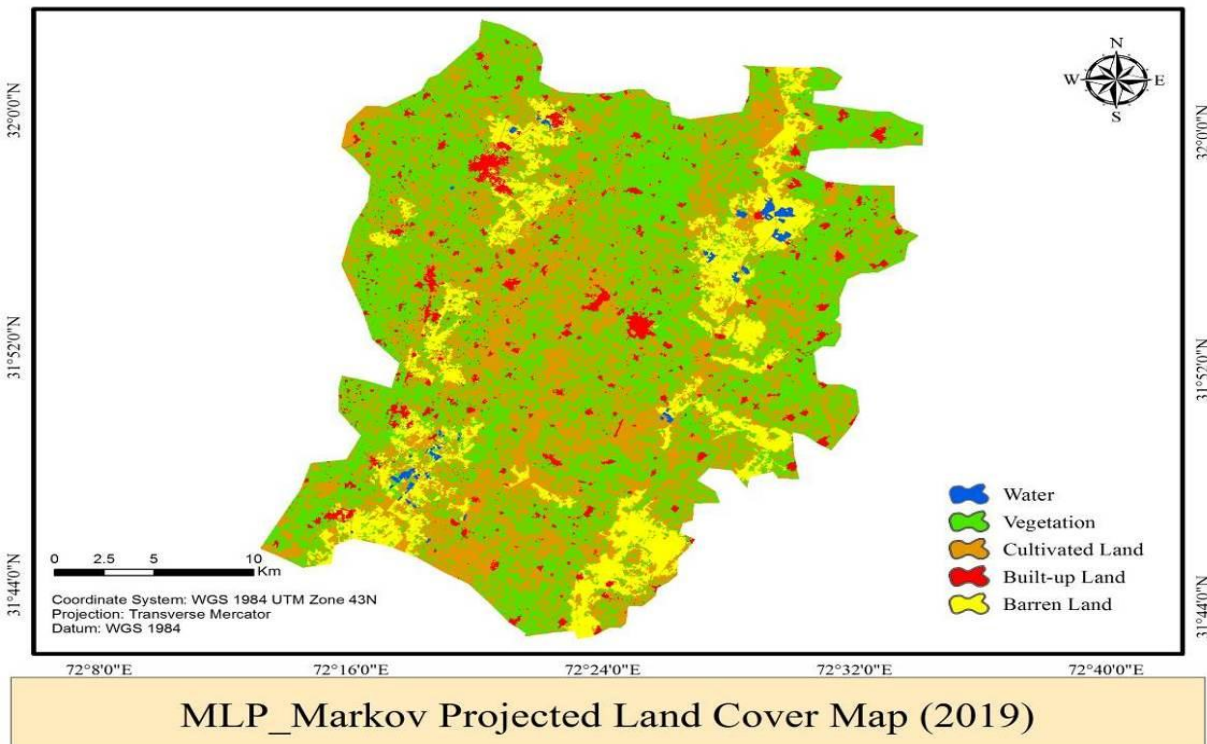


Figure 9: MLP_Markov Projected Landuse/LandCover Map For Year 2019

Conclusion:

The aim of this research work was to analyze the growth of Built-up land and its impact on other classes. Different techniques and tools of remote sensing and geographical information system were used. For LULC maps, five classes were extracted but the emphasis was given to built-up area. Built-up land showed a growth of 1.18 % from 1999 to 2009 all around the tehsil while 0.38% from 2009 to 2014. CA_MARKOV and MLP_MARKOV model had been implemented for projecting the LULC change for 2014. The projected images for the year 2014 resulted from

both models were validated by kappa statistics and compared with LULC map of 2014, CA_MARKOV simulated all classes while MLP_MARKOV only simulated only built-up land based on driving variables and transition potential maps. Results showed that both models have the good quantitative agreement for built-up land and barren land but for vegetation, cultivated land and water the agreement was poor. MLP_MARKOV showed relatively good agreement for the amount of area and spatial similarity in the case of built-up land. In projected image of 2019, the built-up area raised along the road at Sahiwal city suburbs and around the city which might degrade the vegetation. In the rural area of Sahiwal, vegetation, and cultivated land may also be affected by increasing built-up land in projected image. Thus final remote sensing and geographical information system, both have the potential to map the LULC classes as compare to other methods. These technologies are able to model different scenarios in different periods.

References

- [1] B. Turner, W. B. Meyer, and D. L. Skole, "Global land-use/land-cover change: towards an integrated study," *AMBIO-STOCKHOLM*-, vol. 23, pp. 91-91, 1994.
- [2] M. W. a. T. I. BL, *Changes in landuse and landcover: A global perspective*. Cambridge: A global perspective. Cambridge Univ. Press, 1991.
- [3] U.N.F.A.O, "United Nation Food and Agricultural Organization," Online Journals. Nigerian National Population Commission (2006) 1997.
- [4] G. N. C. E. R. Narayanan, "Satellite remote sensing techniques for natural resources survey," In *Environmental Management*, edited by L-R Singh, Savindra Singh, R C Tiwari and R P Srivastava (Allahabad geophysical society), pp. 177-181, 1983.
- [5] O. a. Poonam, "Urban Sprawl Mapping and Landuse Change Detection Using Remote Sensing and GIS," *International Journal of Remote Sensing and GIS*, vol. Volume 1, pp. 12-25, 2012.
- [6] Ezeomedo and J. Igbokwe, "MAPPING AND ANALYSIS OF LANDUSE AND LANDCOVER FOR A SUSTAINABLE DEVELOPMENT USING MEDIUM RESOLUTION SATELLITE IMAGES AND GIS," *International Journal of Engineering & Management Sciences*, vol. 3, 2012.
- [7] UNFPA.(2008).Available: <http://www.unfpa.org/swp/2007/english/introduction.html>
- [8] J. T. F. David S. Wilkie, *Remote Sensing Imagery for Natural Resources Monitoring*. New York: COLUMBIA University Press, 1996.
- [9] M. M. Elaalem, Y. D. Ezlit, A. Elfghi, and F. Abushnaf, "Performance of Supervised Classification for Mapping Landcover and Landuse in Jeffara Plain of Libya," *International Proceedings of Chemical, Biological & Environmental Engineering*, vol. 55, 2013.
- [10] Q. Zhou, "The integration of GIS and remote sensing for land resource and environment management," in *Proceedings of United Nation ESCAP Workshop on Remote Sensing*

- and GIS for Land and Marine Resources and Environmental Management, 1995, pp. 13-17.
- [11] S. Hathout, "The use of GIS for monitoring and predicting urban growth in East and West St Paul, Winnipeg, Manitoba, Canada," *Journal of Environmental management*, vol. 66, pp. 229-238, 2002.
- [12] J. R. Jensen and D. C. Cowen, "Remote sensing of urban/suburban infrastructure and socio-economic attributes," *Photogrammetric engineering and remote sensing*, vol. 65, pp. 611-622, 1999.
- [13] T. Lasanta, S. Beguería, and J. M. García-Ruiz, "Geomorphic and hydrological effects of traditional shifting agriculture in a Mediterranean mountain area, Central Spanish Pyrenees," *Mountain Research and Development*, vol. 26, pp. 146-152, 2006.
- [14] J. T. Al-Bakri, M. Ajlouni, and M. Abu-Zanat, "Incorporating landuse mapping and participation in Jordan: An approach to sustainable management of two mountainous areas," *Mountain Research and Development*, vol. 28, pp. 49-57, 2008.
- [15] M. F. Jasinski, "Estimation of subpixel vegetation density of natural regions using satellite multispectral imagery," *Geoscience and Remote Sensing, IEEE Transactions on*, vol. 34, pp. 804-813, 1996.
- [16] H. Mahmoodzadeh, "Digital change detection using remotely sensed data for monitoring green space destruction in Tabriz," *International Journal of Environmental Research*, vol. 1, 2007.
- [17] Ruiz-Luna and C. A. Berlanga-Robles, "Landuse, landcover changes and coastal lagoon surface reduction associated with urban growth in northwest Mexico," *Landscape Ecology*, vol. 18, pp. 159-171, 2003.
- [18] M. G. a. C. L. R. Turner, "Change in landscape patterns in Georgia, USA," *Landscape Ecology*, vol., pp. 421-251, 2004.
- [19] G. P. A. R. S. DeFries, and R. A. Houghton, *Ecosystems and Landuse Change*. Washington D.C.: American Geophysical Union, (2004).
- [20] T. H. a. L. H. M, "Modeling and projecting land-use and land-cover changes with a cellular automaton in considering landscape trajectories An improvement for simulation of plausible future states," in *EARSeL eProc*, ed, 2006, pp. 63–76.
- [21] www.neims.com.pk. Landuse Atlas of Pakistan.
- [22] Z. E. N, "Cellular Automata," in *The Stanford Encyclopedia of Philosophy*, ed, 2012.
- [23] P. Cabral and A. Zamyatin, "Three land change models for urban dynamics analysis in Sintra-Cascais area," in *Proceedings of First Workshop of the EARSEL SIG on Urban Remote Sensing: Challenges and solutions*, 2006.
- [24] J. R. Eastman, "IDRISI Taiga guide to GIS and image processing," Clark Labs Clark University, Worcester, MA, 2009.
- [25] J. Eastman, "IDRISI taiga Tutorial," Worcester: Graduate School of Geography, Clark University. 333p, 2009.
- [26] C. U. Clark Labs, 950 Main Street, and M.-. Worcester. IDRISI Taiga Help System Available: http://www.clarklabs.org/support/upload/IDRISI_Taiga_Help.zip,

- [27] Multilayer Perceptron. (n.d.). In Wikipedia. Available: http://en.wikipedia.org/wiki/Multilayer_perceptron
- [28] J. Van Vliet, A. Hagen-Zanker, G. Engelen, J. Hurkens, R. Vanhout, and I. Uljee, "Map Comparison Kit 3: User Manual," Maastricht: Research Institute for Knowledge Systems, 2009.